Economic Geology
Vol. 96, 2001, pp. 1055–1072

Hydrothermal Alteration and Volatile Element Halos for the Rosebery K Lens Volcanic-Hosted Massive Sulfide Deposit, Western Tasmania

ROSS R. LARGE,† RODNEY L. ALLEN,* MICHAEL D. BLAKE, AND WALTER HERRMANN

Centre for Ore Deposit Research, School of Earth Sciences, University of Tasmania, GPO Box 252-79, Hobart, Tasmania 7001, Australia

Abstract

A detailed study of alteration mineralogy, mineral chemistry, and lithogeochemistry in the host rocks surrounding the A-B and K lenses at the north end of the Rosebery mine has revealed a series of overlapping alteration halos with characteristic mineralogy and geochemistry. The study involved logging and sampling from nine drill holes spaced at varying distances from the A-B and K lenses. The stratiform Zn-Pb-Cu ore lenses have a sheetlike morphology and are hosted by a mixed sequence of rhyolitic to dacitic massive medium-grained quartz-porphyritic pumice breccia, black mudstone, and crystal-rich volcaniclastic sandstone, overlying a thick homogeneous sequence of rhyolitic pumice breccia.

The major alteration minerals at Rosebery are arranged in a complex series of zones passing away from the deposit—quartz-sericite zone, Mn carbonate zone, chlorite zone, and outer sericite zone. The chlorite zone is best developed in the immediate footwall below the copper-pyrite-rich ore lenses, whereas the strongest Mn carbonate alteration occurs in the immediate hanging-wall volcanics or lateral to the ore lenses. The outermost visible sericitic alteration extends about 60 to 100 m into the footwall, 10 to 20 m into the hanging wall, and over 500 m along the upper contact of the footwall pumice breccias.

Thallium and antimony form the most extensive trace element halos related to the mineralization. Thallium forms a halo that extends 200 to 300 m into the overlying volcanics and 60 to 100 m into the footwall. Anomalously high thallium also occurs over 500 m along strike marking the contact between the footwall pumice breccias and the overlying volcaniclastic sandstones. Proximal to the ore lenses Tl and Sb values range from 10 to 100 ppm, compared to the halo zone where they vary from around 1 to 10 ppm.

Studies of alteration mineral chemistry at Rosebery have revealed some important relationships that may assist exploration. The Mn content of alteration carbonate increases toward ore, both along strike and across strike. Close to ore, alteration carbonates contain >20 mole percent $MnCO_3$ (kutnahorite, rhodochrosite, Mn siderite, and Mn ankerite), whereas at distances of 40 to 60 m across strike the mole percent $MnCO_3$ in carbonate drops to below 10 percent. At greater than 80 m, the carbonates are Mn-poor calcites and are commonly located in synmetamorphic structures. White mica composition changes with stratigraphy and alteration assemblages and may be related to the mineralizing event, although this has not been convincingly demonstrated. Proximal white mica contains minor Ba substituting for octahedral Al. However, except for their Ba content, these phengetic white micas are similar to those found in nonmineralized areas of the Mount Read Volcanics. Sodic white mica with up to 0.35 Na/(Na + K) and a low phengite content (<0.5 Fe + Mg cations) occurs in a zone of volcanic sandstones and black slates overlying the ore deposit.

This research has lead to the development of a series of proximal, medial, and distal vectors useful for both regional and mine-scale exploration. The most useful vectors, listed from proximal to distal, include Zn, Ba content of white mica, Na_2O, K_2O, Ishikawa alteration index (AI), S/Na_2O, Ba/Sr, Mn content of carbonate, Tl, and Sb.

Introduction

THE ROSEBERY massive sulfide deposit is a major sheet-style polymetallic Zn-Pb-Cu-Ag-Au volcanic-hosted massive sulfide (VHMS) deposit within the Mount Read Volcanics of western Tasmania (Fig. 1; Green et al., 1981; Large, 1992). The global mining resource of the deposit is 28.3 million metric tons (Mt) at 14.3 percent Zn, 4.5 percent Pb, 0.6 percent Cu, 145 g/t Ag, and 2.4 g/t Au (P. Edwards, pers. commun., 1998). Unlike the Hellyer deposit to the north, which consists of one major elongate ore lens (Gemmell and Fulton, 2001), Rosebery is made up of 16 separate ore lenses (Fig. 2), which vary in size from 0.1 to 5 Mt. Because of the composite lens nature of the orebody, the future of the Rosebery mining operation has depended on the continual discovery of new ore lenses in order to maintain the required feed to the mill. This, in turn, has depended on the continual development and upgrading of in-mine exploration techniques, including geology, geochemistry, and geophysics, to enable the required discovery rate to be maintained. The importance of being able to predict the presence of new ore lenses within the mine environment has thus become a driving factor for research at Rosebery. With this in mind, the current study was undertaken to characterize the lithogeochemical alteration halo surrounding one of the major ore lenses and to develop lithogeochemical vectors that may be useful in the exploration for new ore lenses.

Rosebery is one of five major VHMS deposits within the Cambrian Mount Read Volcanics belt of western Tasmania (Fig. 1). The deposit formed late in the volcanic history of the belt, associated with a period of Middle Cambrian east-west extension, followed by Late Cambrian north-south folding and basin inversion (Berry and Keele, 1997). Detailed geology of the Rosebery mine is provided by Green et al. (1981), Green and Iliff (1989), and Khin Zaw et al. (1999) and will not

†Corresponding author: e-mail, Ross.Large@utas.edu.au
*Present address: Volcanic Resources Limited, Boliden Mineral AB, 93681 Boliden, Sweden.

0361-0128/01/3172/1055-18 $6.00

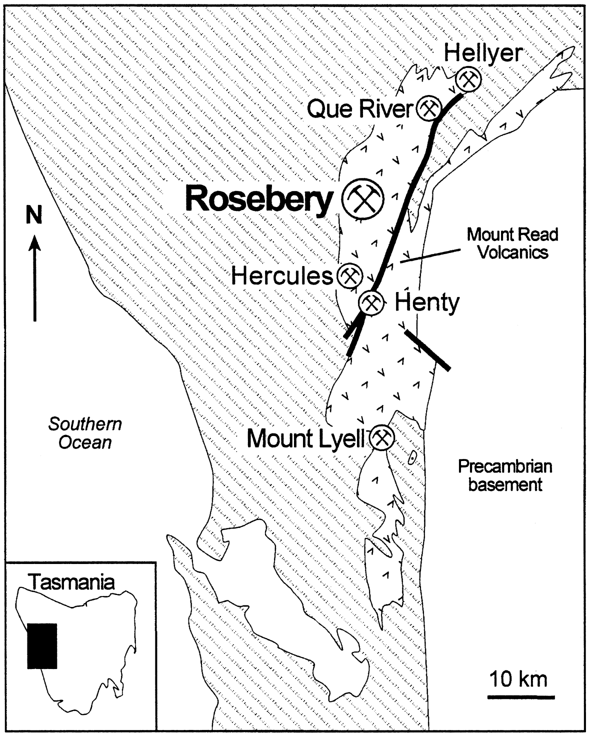

FIG. 1. Location diagram showing Rosebery and the other major VHMS deposits in the Mount Read Volcanics, western Tasmania.

be repeated here. The 16 ore lenses occur along a strike length of over 2,000 m (Fig 1). The stacked stratiform lenses have undergone at least two phases of Devonian deformation, including tight folding (Brathwaite, 1972) and thrust faulting (Berry and Keele, 1997). The combination of folding and thrusting has resulted in a complex pattern of ore lenses and alteration (e.g., Large, 1990, fig. 6) in the southern end of the mine between 500mN and 500mS (Fig 1). In comparison the ore lenses in the northern end of the mine from 550mN to 1700mN show less effects from the deformation (Huston and Large, 1988) and have thus been chosen for this alteration study.

In the northern end, the sulfide ore lenses have an average thickness of 2 to 10 m, a strike length of 100 to 400 m (Fig. 3), and a downdip extent of 100 to 500 m. The principal ore lens mineralogy is sphalerite, galena, pyrite, chalcopyrite, tetrahedrite, with lesser arsenopyrite and pyrrhotite. Dominant alteration minerals are sericite, chlorite, Mn carbonates, barite, and quartz. Metamorphic grade is lower greenschist facies.

Most previous workers have considered the Rosebery ore lenses to be synvolcanic exhalative in origin (e.g., Braithwaite, 1974; Green et al., 1981; Huston and Large, 1988; Green and Iliff, 1989; Large, 1992; Khin Zaw et al., 1999). However, recent work by Allen (1994b) provides evidence for a synvolcanic subsea-floor replacement origin for at least some of the massive sulfide lenses.

Volcanic Host Rocks

The lowest stratigraphic unit exposed in the Rosebery-Hercules area is a poorly stratified, rhyolitic pumice deposit of greater than 800-m thickness, with subordinate coherent to hyaloclastic sills (footwall volcanics; Allen, 1994a). These are overlain by a well-stratified, up to 300-m thick, succession of black mudstone and rhyolitic pumiceous mass-flow units (Fig. 3; hanging-wall volcaniclastics). These are in turn overlain by a more than 1-km-thick sequence of rhyolitic pumice breccias, lavas, and dacitic intrusions known informally as the Mount Black volcanics (Allen, 1994a; Gifkins and Allen,

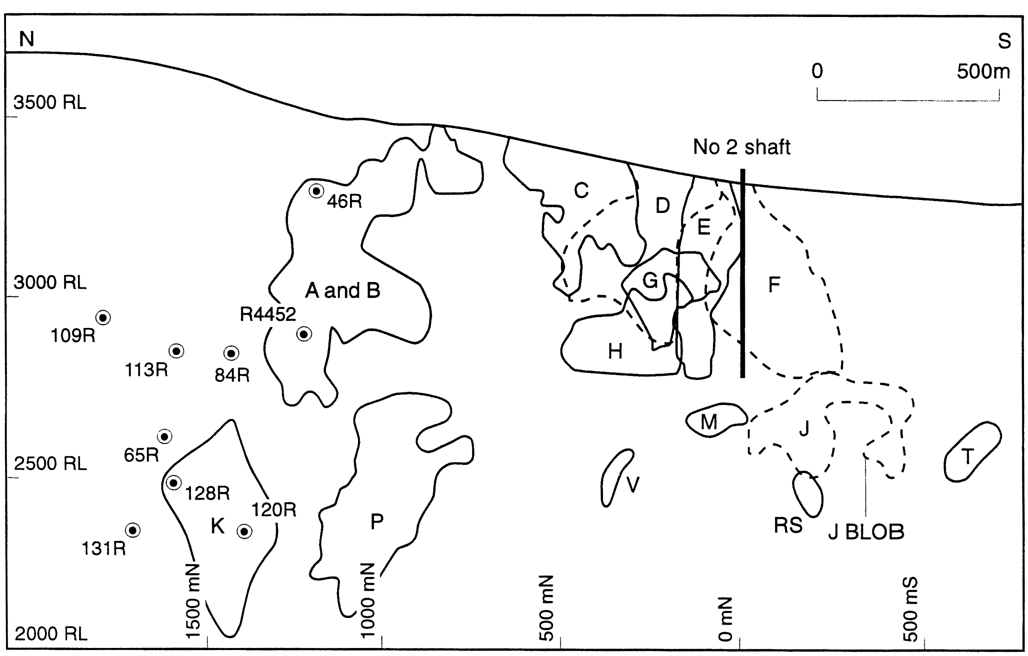

FIG. 2. Long section of the Rosebery mine, showing the outlines of the 16 major ore lenses and the locations of the drill holes sampled in this investigation.

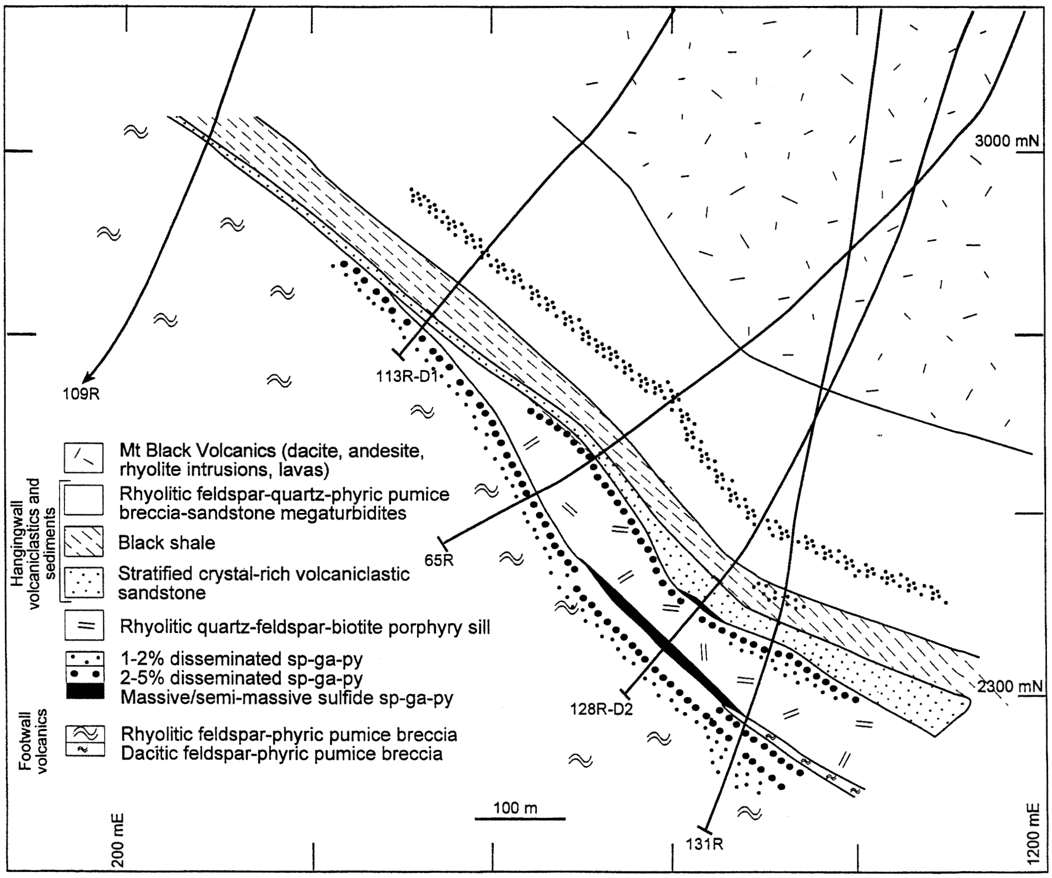

FIG. 3. Geologic cross section, Rosebery mine at 1700mN, showing the relationship of the ore lenses to host rocks.

2001). Locally, a 0- to 50-m-thick package of stratified, felsic, crystal-pumice-lithic sandstones and siltstones occurs at the boundary between the footwall volcanics and hanging-wall volcaniclastics (Fig. 3). This package is termed "host rock" by Rosebery mine staff and is here called the "volcaniclastic sandstone unit."

The pumiceous units of the footwall volcanics and hanging-wall volcaniclastics are mainly interpreted as submarine mass-flow deposits, which were fed directly (syneruptively) from large, subaerial to shallow-water, pyroclastic eruptions (Allen and Cas, 1990; Allen, 1994a). The footwall volcanics pumice breccia is interpreted to have ponded within a large caldera subsidence structure, which subsided during eruption of the pumice breccia (Green et al., 1983; Allen, 1994a). The volcaniclastic sandstone unit is interpreted mainly as slightly to moderately reworked pyroclastic debris, derived mainly from the footwall volcanics pumice deposit (Allen, 1994a).

Sampling and Analysis

A total of 255 samples were collected and analyzed from nine drill holes at the northern end of the Rosebery deposit (Fig. 2). Four of the drill holes intersect the ore lenses (DDH 120R, 128R, R4452, and 46R), and the other five intersected the host stratigraphy at varying distances west of the ore lenses, from 100 to 500 m west (DDH 131R, 65R, 84R, 113RDI, and 109R). Where possible samples were collected over a stratigraphic thickness of 500 m from the footwall volcanics, through the host rock volcaniclastic sandstones, the hanging-wall volcaniclastics, and up to the base of the Mount Black volcanics.

All samples were analyzed for the major elements, including S, by X-ray fluorescence (XRF). Trace elements were analyzed by XRF or ICP-MS according to the following scheme: XRF: As, Ba, Ce, Cr, Cu, La, Nd, Ni, Pb, Rb, Sc, Sr, Th, V, Y, Zn, and Zr; ICP-MS: Ag, As, Bi, Cd, Cs, Mo, Sb, Tl, and U.

XRF analyses were performed at the University of Tasmania on a Philips PW1480 spectrometer, using a fusion disk method for major elements (0.77-g sample, 4.125-g flux, i.e., 1:5.4 sample to flux ratio) and pressed powder pills (10-g sample) for trace elements. Precision for major elements was ±1 percent and generally 1 to 5 percent for trace elements except near the detection limit (1–4 ppm) where it could be 20 to 30 percent, depending on the element. Detection limits (in ppm) for the XRF in a silicate matrix were As (4), Ba (4), Ce (4), Cr (1), Cu (1), La (2), Nd (2), Ni (1), Pb (1.5), Rb (1), Sc (2), Sr (1), Th (1.5), V (1.5), Y (1), Zn (1), and Zr (1). Numerous international rock reference materials were run to check the accuracy of the methods. ICP-MS analyses were done by Analabs Laboratories (Australia) with detection limits (in ppm) of Ag (0.1), As (1), Bi (0.2), Cd (0.1), Cs (0.05), Mo (0.1), Sb (0.5), Tl (0.5), and U (0.05). A mixed acid digestion of aqua regia, perchloric, and hydrofluoric acid was used. Precision was generally better than ±10 percent, although near the detection limit ±20 to 50 percent. Fifteen international rock reference materials were also submitted to check the accuracy of the analyses.

Each analyzed sample represents half drill core about 15 cm in length. In addition to chemical analysis, each sample was studied petrographically and by portable infrared mineral analyzer (PIMA) to document mineralogy and textures. Alteration mineral compositions were determined for an additional 15 percent of the samples, using electron microprobe methods.

Chemostratigraphy

Immobile element ratios can be used to assist volcanic stratigraphic interpretation in complex volcanic sequences, especially close to mineralization, where the intensity of hydrothermal alteration makes it difficult to interpret primary lithologies (e.g., Whitford et al., 1989; MacLean and Barrett, 1993; Barrett et al., 1996). Volcanic facies correlations in the nine drill holes sampled in this study have been tested using the downhole Ti/Zr ratio, which is generally a good guide to primary volcanic composition (Crawford et al., 1992; MacLean and Barrett, 1993). This is because Ti and Zr are immobile elements and the Ti/Zr is unaffected by hydrothermal alteration or metamorphism. Previous work by R.F. Berry (unpub. data) and Reid (1993) suggested that a subtle contact between the ore-bearing strata and the footwall rocks could be defined by the Ti/Zr ratios.

Using the Ti/Zr downhole plot from DDH 120R (Fig. 4) as an example, it is apparent that the major stratigraphic contacts are marked by abrupt changes in Ti/Zr. This indicates that each stratigraphic unit is characterized by a different volcanic composition. By plotting TiO_2 against Zr for the feldspar-porphyritic pumice breccias that underlie and locally enclose the ore (Fig. 5a), it is possible to show that, athough the samples are altered and therefore have variable Ti and Zr contents, they fall into two groups, each with a consistent Ti/Zr ratio, plotting along lines that extend through the origin (see discussion by MacLean and Barrett, 1993). This suggests that although the pumice breccias are strongly altered, they represent two compositionally distinct units, a feature that is only apparent in the geochemistry and was not discernible in the drill core logging program or the thin section petrography.

In Figure 5b samples from the quartz-feldspar-biotite porphyritic sill that overlies the Rosebery K lens are shown to plot along the same line (Ti/Zr ratio of 12–14) as those from the upper feldspar-porphyritic pumice breccia. This suggests that although both the pumice breccia and the porphyritic sill have different phenocryst mineralogies, they are both slightly more mafic in composition than the footwall pumice breccias, which are distinctly rhyolitic, with a Ti/Zr = 7 to 9. This suggests that toward the end of the huge rhyolitic pumice-breccia eruption that formed the Rosebery footwall, the eruption tapped a less felsic magma. Possibly the source magma chamber was chemically zoned (as is typical of many large magma chambers), and toward the end of the eruption, rhyolite at the top of the chamber became exhausted and an underlying more mafic magma was erupted. Our recent research suggests that the quartz-feldspar-biotite porphyritic sill is a member of a regionally extensive series of sills emplaced soon after the footwall pumice breccias.

The volcaniclastic sandstones and siltstones overlying the pumice deposits have variable Ti/Zr ratios from 10 to 30, indicating a mixed and variable composition suggestive of a mixed felsic and mafic provenance. This is consistent with the interpretation that these rocks represent a reworked facies. The black slate in DDH 120R exhibits much higher Ti/Zr ratios, from 30 to 40 (Figs. 4, 5), probably resulting from separation of Ti from Zr during sedimentary processes, leading to concentration of Ti in the clay-rich fraction of the black mudstones (e.g., Goodfellow and Peter, 1994). The uppermost volcaniclastic mass flows also exhibit a variable Ti/Zr ratio. Typically the Ti/Zr ratio decreases upward in each normal graded, subaqueous mass-flow unit. Consequently, the variable Ti/Zr ratio probably reflects the physical fractionation of crystals and lithics from pumice and shards during deposition of each bed.

In summary, the Rosebery ore lenses occur at the top of a thick pile of rhyolitic pumice breccias, probably representing a submarine caldera eruption (Allen, 1994a). The stratigraphic interval of mineralization coincides with the onset of more mafic volcanism contributing to a mixed sequence of dacitic pumice breccias, reworked volcanics, and quartz-porphyritic sills. The mineralized stratigraphic interval is followed by a period of nonvolcanic sedimentation represented by the hanging-wall black mudstones.

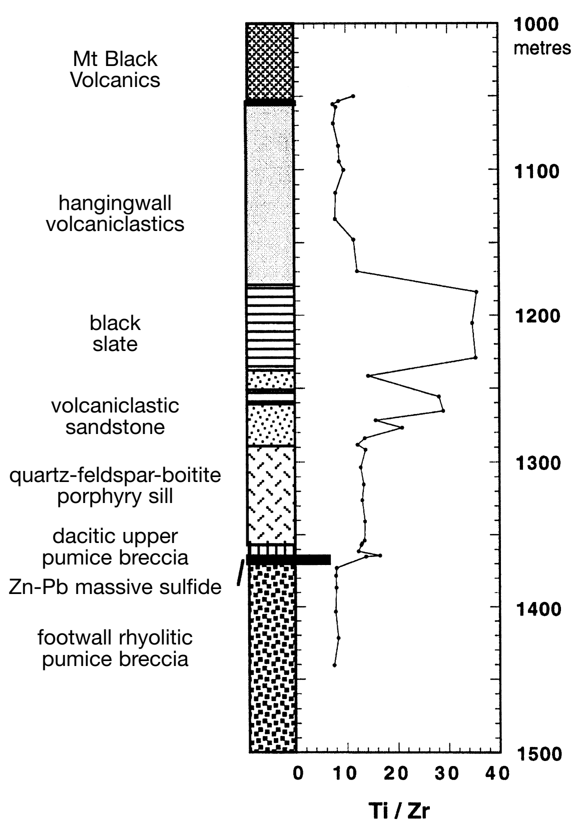

FIG. 4. DDH 120R, downhole plot of Ti/Zr ratio compared to stratigraphy determined from drill hole logging. Note the steps in the Ti/Zr ratio at the major stratigraphic boundaries.

Alteration Mineralogy and Zonation

Previous studies (Green et al., 1981; Naschwitz and Van Moort, 1991) have characterized the mineralogy and geochemistry of

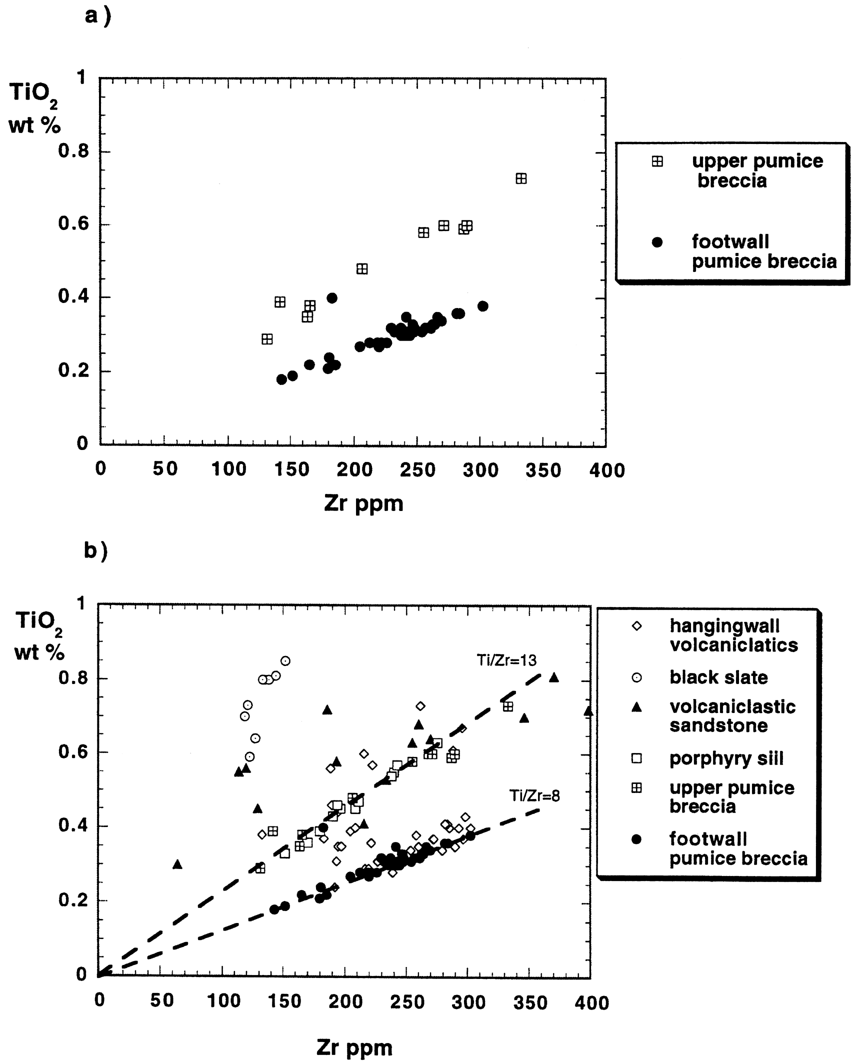

FIG. 5. a. Relationship between TiO_2 and Zr for the pumice breccias at the Rosebery K lens. This graph indicates two compositional types: the upper pumice breccia has a higher Ti/Zr ratio (13), indicating a more mafic composition, relative to the major footwall pumice breccia. b. Relationship between TiO_2 and Zr for all of the major lithologies at Rosebery, showing the different trends relating to varying Ti/Zr ratios for each lithology.

the broad-scale wall-rock alteration associated with Rosebery ore lenses. Extensive zones of quartz-sericite alteration have been defined in the footwall volcanic succession below the ore lenses, compared to weak or nonexistent alteration in the hanging-wall volcaniclastics. Unlike many other VHMS deposits, no chlorite-rich footwall alteration pipes have been located at Rosebery; however, restricted strata-bound chlorite-pyrite zones have been recorded below the more copper-rich ore lenses (Brathwaite, 1974; Green et al., 1981) in the south end of the mine, which possibly represent high-temperature fluid vents. A detailed description of the sequence of alteration events at Rosebery is provided by Allen (1997), where he shows that early clay, zeolite, K feldspar diagenetic alteration is overprinted by the hydrothermal ore-related carbonate, sericite, quartz, chlorite, sulfide mineral assemblages. Subsequent deformation events during the Devonian gave rise to calcite, albite, chlorite, epidote, magnetite, leucoxene-bearing assemblages that were overprinted by granite-related alteration assemblages, which include biotite, tourmaline, chlorite, magnetite, carbonate, fluorite, and arsenopyrite (Khin Zaw, 1994).

Downhole alteration mineral variation

Mineralogical changes associated with hydrothermal alteration have been studied in relationship to established chemostratigraphy in DDH 120R, which intersected the center of the K lens (Fig. 4). A mineral percentage bar chart for a series of samples through the stratigraphic host sequence is shown in Figure 6. The mineral percentages have been calculated from the whole-rock analyses by the least squares method outlined by Herrmann et al. (2001) and show good agreement with the thin section estimates. Combining the data from Figures 4 and 6 indicates that passing stratigraphically upward through the footwall rhyolitic pumice breccias toward the K lens, albite content decreases, whereas the hydrothermal minerals white mica, quartz, chlorite, and minor

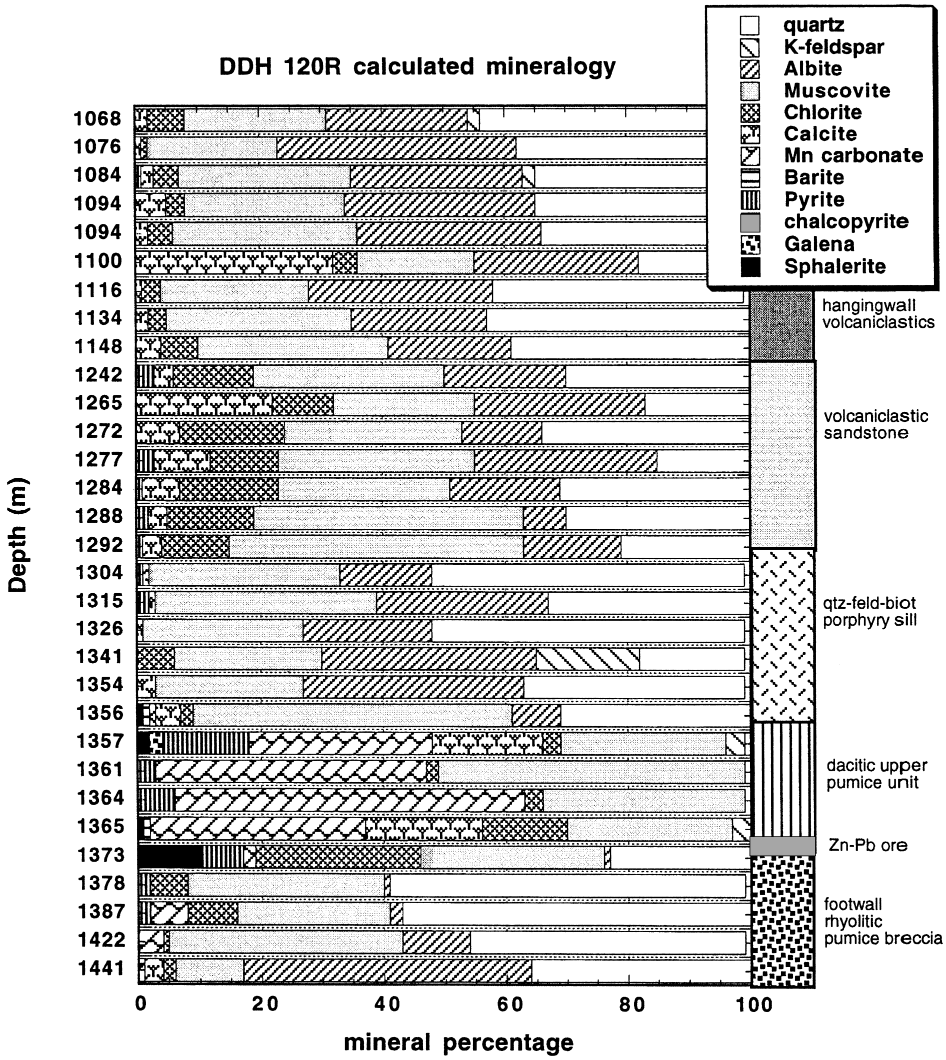

FIG. 6. Variation in mineral abundances in samples from DDH 120R through the K lens.

Mn carbonate increase. Maximum chlorite contents occur immediately below the ore lens, whereas maximum Mn carbonate contents occur directly above or along strike from the ore lens in the upper dacitic pumice unit. At other locations, Mn carbonate is concentrated directly below the ore lens (e.g., DDH R4452).

The basal 4 m of the hanging-wall quartz-feldspar-biotite porphyry sill show intense white mica alteration and albite depletion; however, the central zone of the porphyry sill shows significantly less alteration. The volcaniclastic sandstone unit above the porphyry sill may be moderately to strongly hydrothermally altered in the lower section (samples 1284, 1288, 1292), exhibiting white mica enrichment and albite depletion, and intervals of calcitic carbonate impregnation are common. Hanging-wall rocks above 1,280 m (i.e., 90 m above the ore lens) show no strong mineralogical effects of hydrothermal alteration, except for scattered strata-bound zones of calcite impregnation and weak sericite and chlorite development. Chlorite and calcite enrichment in the hanging-wall volcaniclastic sandstone unit could in part be a primary compositional feature related to the greater abundance of feldspar crystals and mafic lithic clasts in this unit.

Alteration mineral zonation

Combining the alteration mineralogy data in DDH 120R (Fig. 6) with similar data obtained from the other eight drill holes studied (Fig. 2) enabled the development of a simple alteration zonation model for the K lens (Fig. 7), which comprises four major zones: a quartz-sericite zone, a Mn carbonate zone, a chlorite zone, and a sericite-carbonate zone.

Quartz-sericite zone: Massive and semimassive sulfides mainly occur in one or more strataparallel zones of bleached quartz-sericite sulfide composition (Fig. 7). Rock textures vary from homogeneous to spotty and augen schist textured, the latter comprising an anastomosing fabric of strongly foliated sericite > quartz domains wrapping around siliceous knots of quartz > sericite. At the lateral margins of ore-grade mineralization, the quartz-sericite zone continues with 1 to 10 percent disseminated sulfides (pyrite, sphalerite, galena). The sulfides preferentially occur in the siliceous spots or augen.

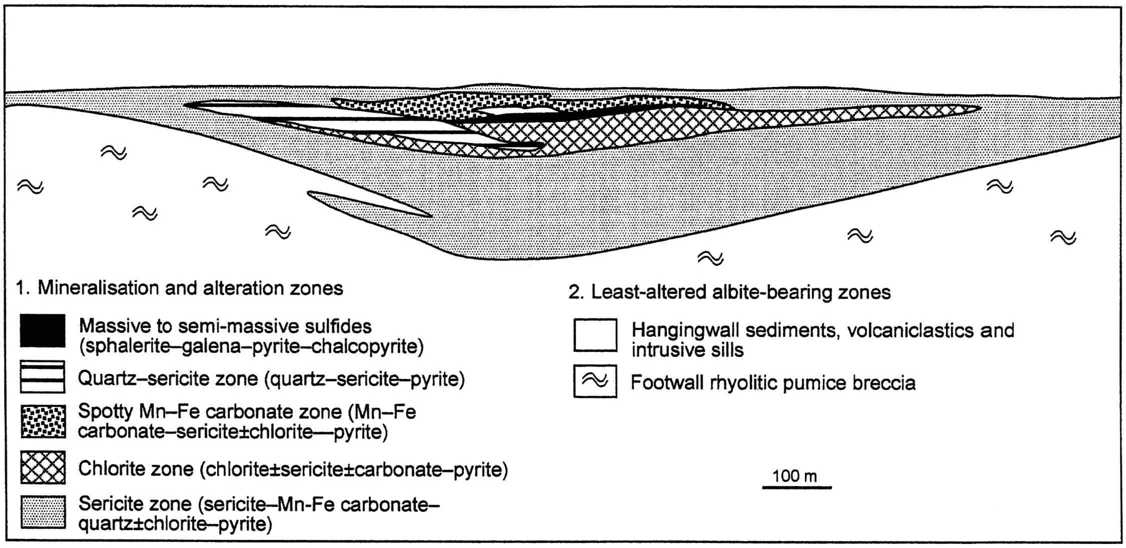

FIG. 7. Diagrammatic model of alteration mineral zones surrounding the K lens, Rosebery.

Mn carbonate zone: The mineralized quartz-sericite zone is overlain (e.g., DDH 120R) and/or locally underlain (e.g., DDH R4452) by a zone of intense Mn-bearing carbonate alteration up to 10 m thick. Intense Mn carbonate is closely associated with massive sulfide but locally extends several tens of meters beyond the limits of known massive sulfide (e.g., downdip of the K lens intersection in section 1700 mN, Fig. 3). The Mn carbonate typically has a spotty texture, comprising 25 to 60 percent Mn carbonate spots in a sericitic, or locally chloritic, matrix. This alteration zone is generally poor in sulfides.

Chlorite zone: Chlorite is concentrated in the immediate footwall of the ore lenses, varying in content from 15 to 50 wt percent. Thickness of the intense chlorite alteration is generally less than 5 m in the drill holes studied. The thickest and most intense chlorite alteration exists in footwall zones to the copper-rich lenses elsewhere at Rosebery, particularly the south-end ore lenses. A narrow zone of chlorite alteration extends along strike in the footwall of the ore position at the K lens (Fig. 7).

Sericite-carbonate zone: A broad alteration zone of sericite with scattered Mn-bearing carbonate blebs overlaps and extends beyond the chlorite, Mn carbonate, and chlorite zones (Fig. 6). White mica content varies from 20 to 60 wt percent through this zone. Distinct sericite-carbonate alteration can be mapped by eye and chemical composition along the ore position (upper contact of footwall pumice breccia) beyond the limit of sampling, i.e., at least 500 m west of the A-B lens and updip from the K lens.

Halo Geochemistry

Previous alteration geochemical studies by Green et al. (1981) and Naschwitz and Van Moort (1991) have demonstrated that certain elements (particularly Si, K, Rb, Mg, Mn) are enriched within the alteration zones close to the deposit and other elements (Na, Ca, Sr) are commonly strongly depleted. Pwa et al. (1992) also showed that Rosebery has a well-defined surface geochemical halo of Ba, Mn, Fe, and F, which is much larger than the mineralogical alteration zone.

In this study, we aimed to define the geochemical variation surrounding the K lens to determine which elements, or ratios of elements, were the most useful for in-mine exploration aimed at finding new ore lenses.The geochemical data from the nine drill holes studied has been presented as downhole plots (e.g., Fig. 8) and in a composite cross section at 1700 mN (Figs. 9 and 10). Not all data have been presented due to space restrictions but are available from the first author on request. Some of the most noteworthy geochemical halo patterns evident from these figures are discussed below.

Zinc, lead, and copper distribution (Figs. 8a, b, c, and 10a, b)

The distinctly ore-related zinc and lead halo is of limited extent, reaching about 400 m along the potential ore position (top of pumice breccias) and only about 20 to 50 m across strike into the footwall. Copper shows a similar pattern to zinc and lead, however, of lower tenor and less strike extent. A poorly defined zone of disseminated sphalerite (100–1,000 ppm zinc) occurs in the hanging-wall volcaniclastics above the quartz-porphyriticsill. A more extensive study is required to determine whether this hanging-wall zinc anomaly is spatially related to the Rosebery orebody or whether it is a regional zinc anomaly within the hanging-wall mass-flow succession. However, the occurrence of widespread zinc enrichment above a major zinc deposit is most likely to be more than coincidence, and we suggest that this halo is worthy of further consideration in the future. This hanging-wall zinc zone is not accompanied by anomalous lead or copper.

Manganese distribution (Figs. 8d and 10c)

Manganese forms a restricted halo, confined to the Mn carbonate alteration zone and the inner parts of the sericite-carbonate zone, which tend to be richer in Mn carbonate blebs. Minor manganese extends further into the footwall sericite alteration zone but exhibits background values (<0.5 wt %) throughout the hanging wall and most of the footwall, except

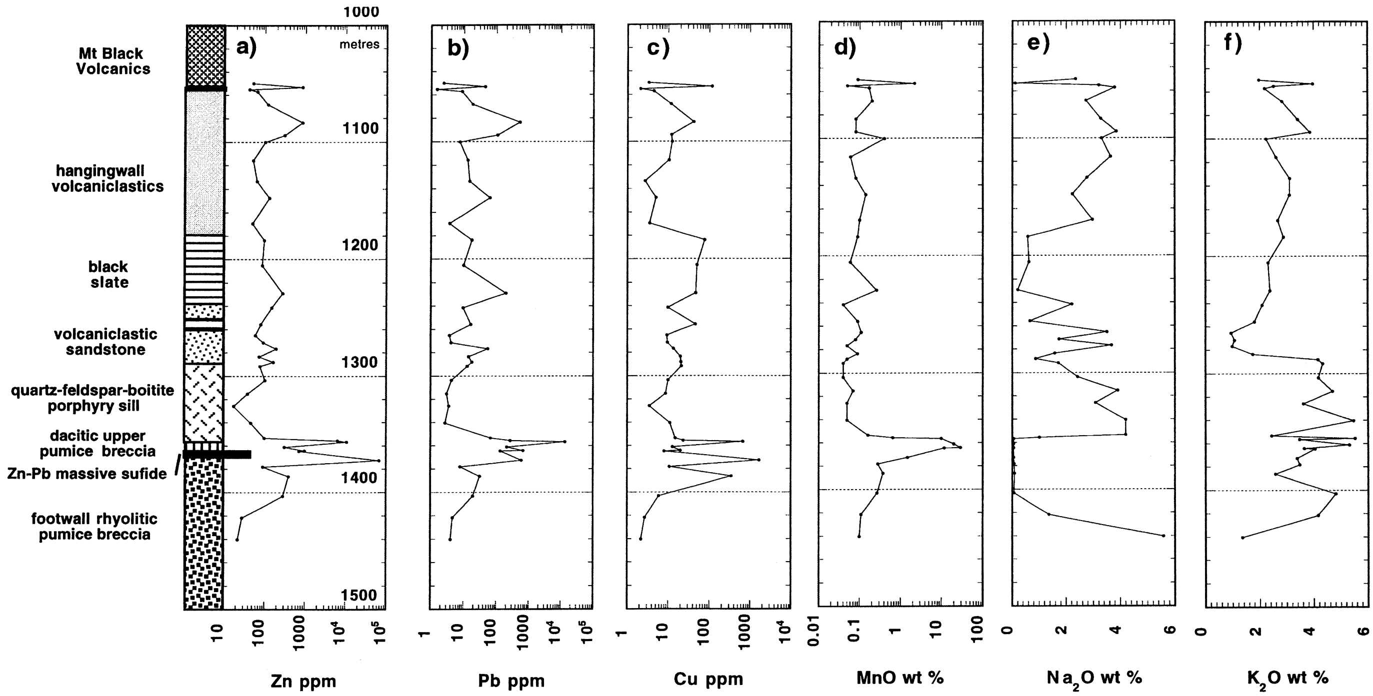

FIG. 8. Downhole geochemical plots for DDH 120R: (a) Zn, (b) Pb, (c) MnO, (d) Na_2O, (e) K_2O.

for local spikes in the downhole geochemical plots that are related to local bleached sericite-carbonate alteration halos around syntectonic and posttectonic veins. For example, the patch of anomalous high manganese deep in the footwall in DDH 109R is related to carbonate-arsenopyrite-pyrite-tourmaline veins with carbonate-bearing halos. Petrographic studies indicate these veins are post- cleavage (Devonian deformation). However carbon and oxygen isotope analyses indicate they have isotopic values similar to the massive sulfide lenses and are distinctly different from Devonian syntectonic granite-related mineralization. They could represent Devonian remobilization of Cambrian alteration-mineralization and may be worthy of further investigation.

Sodium distribution (Figs. 8e and 10d)

Albite replacement by sericite ± chlorite ± quartz has caused a strong sodium depletion (to <0.1 wt %) throughout

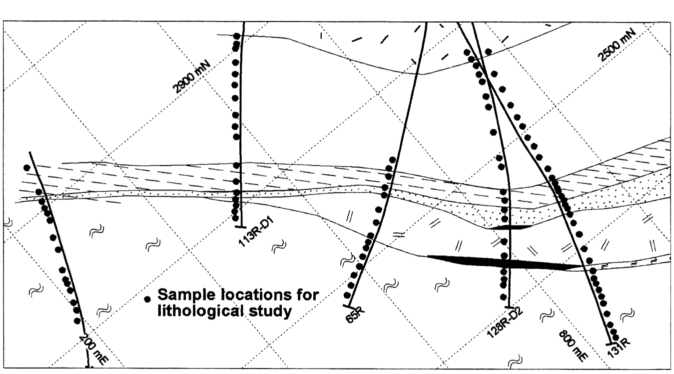

FIG. 9. Sample locations in Rosebery geology cross section 1700 mN. The section in Figure 2 is rotated here for ease of presentation. Geology key is the same as Figure 2.

the footwall alteration zones to the Rosebery ore lenses. This zone thins laterally and grades into a narrow zone of sodium depletion at the top of the footwall pumice breccia, immediately below the potential ore position, for more than 500 m to the west of the A-B and K lenses. Sodium is low in two other zones at Rosebery: along the Black Slate horizon where it is related to primary sedimentary, rather than hydrothermal, processes; and in a narrow zone of sericite ± carbonate, quartz ± sericite and tourmaline alteration along the Mount Black fault (Fig. 2), probably due to the passage of metamorphic fluids along this fault during Devonian deformation and granite intrusion.

Potassium distribution (Figs. 8f and 10e)

Elevated K_2O occurs in a zone surrounding the ore lenses and extending into the overlying quartz-porphyry sill. This envelope of K_2O enrichment (Fig. 8f) is a combination of elevated primary K_2O in the host package (quartz-porphyritic-sill and dacitic pumice breccia) and elevated secondary K_2O related to the intense sericite alteration in the footwall volcanics. The highest levels of K_2O (>5 wt %) occur in a stratabound sericite alteration band about 50 m below the ore lenses. A narrow band of K_2O enrichment also coincides with the sodium depletion zone along the Mount Black fault.

Alteration indexes

A number of alteration indexes and element ratios were tested on the Rosebery data set. Some were found to provide further alteration information and increased the halo dimensions compared to the single element pattern.

Ishikawa alteration index: $(100(MgO + K_2O)/(MgO + K_2O + CaO + Na_2O))$: This index relates to the replacement of plagioclase by sericite and chlorite during hydrothermal

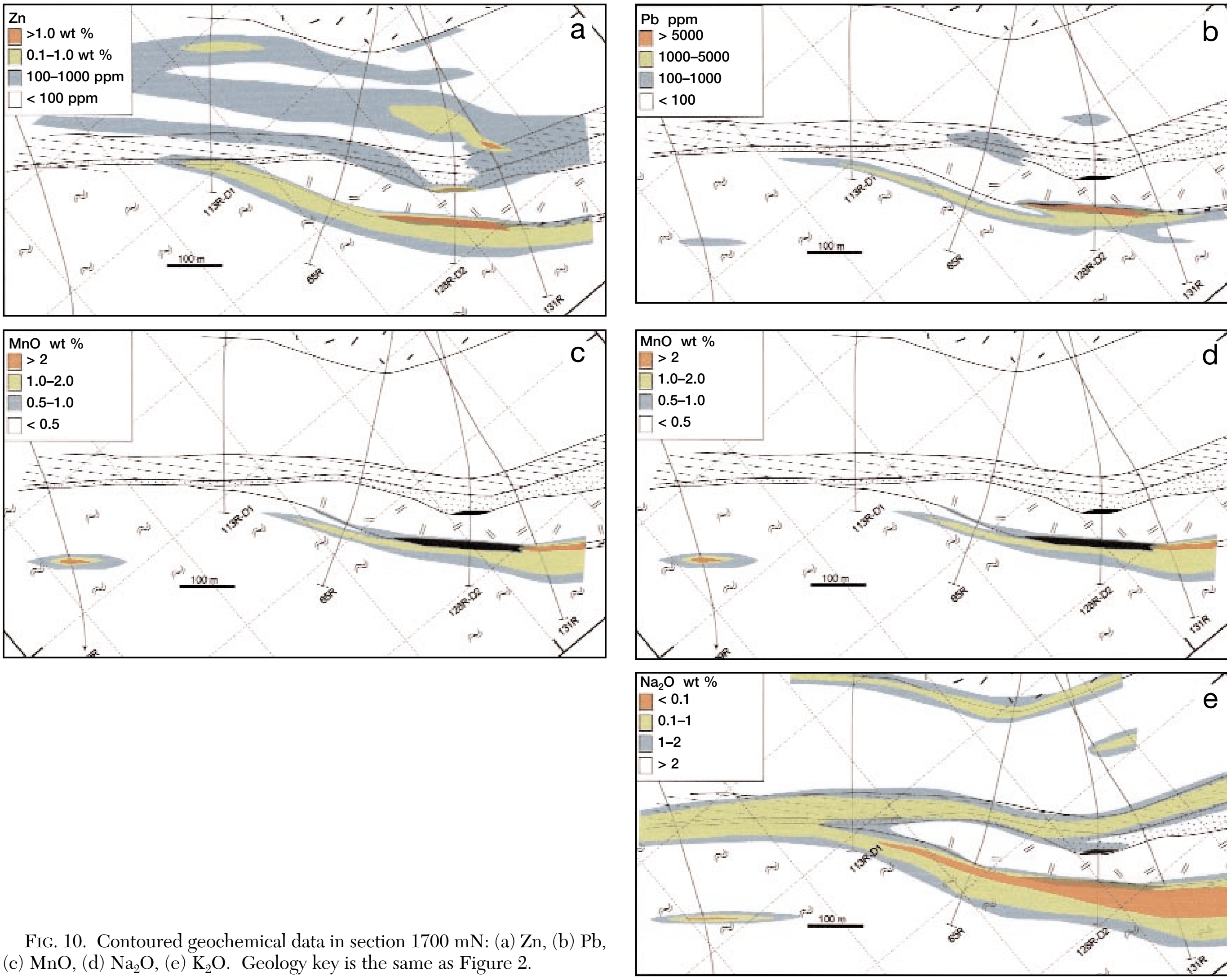

FIG. 10. Contoured geochemical data in section 1700 mN: (a) Zn, (b) Pb, (c) MnO, (d) Na_2O, (e) K_2O. Geology key is the same as Figure 2.

alteration (Ishikawa et al., 1976; Large et al., 2001). The index is elevated to values of 70 to 100 throughout the footwall alteration zone (Fig. 11) and extends along the favorable horizon making an excellent indicator of the ore position (Fig. 11). However at Rosebery the index is unable to detect weak alteration farther into the hanging wall and is unresponsive to carbonate alteration. The index is superior to using Na_2O alone (compare Figs. 10d and 12a) because of its ability to distinguish alkali depletion related to hydrothermal alteration from that related to sedimentary processes (within the Rosebery black slate).

Chlorite, carbonate, pyrite index: (CCPI = 100(FeO + MgO)/(FeO + MgO + K_2O + Na_2O)): This index measures the degree of chlorite, (Fe, Mg) carbonate, and/or pyrite alteration related to VHMS deposits (Large et al., 2001). The index exhibits a systematic increase (from 10–80) through the footwall alteration zone to the ore position (Fig. 11). It is also elevated through the hanging-wall volcaniclastic sandstones and black slate due to the chlorite-carbonate-bearing mineralogy of these sedimentary rocks. This index is less useful due to its variation with primary rock composition and, in the Rosebery data set, is a less distinct vector than S/Na_2O and the Ishikawa alteration index (Fig. 11). The usefulness of the CCPI is demonstrated when it is combined with the Ishikawa alteration index, forming the alteration box plot (Large et al., 2001), to assist in relating alteration mineralogy with alteration geochemistry and zonation in VHMS deposits such as Rosebery.

S/Na_2O ratio: This ratio varies through five orders of magnitude from values of 0.01 in albite-rich, pyrite-poor unaltered volcanics to over 100 for pyrite-rich, albite-depleted highly altered volcanics (Fig. 11). The ratio is an excellent vector within footwall sericite and pyrite-bearing alteration zones and for up to 50 m into the hanging wall but is of little use in weakly developed hanging-wall alteration, which typically lacks significant sulfide development or albite destruction. The ratio provides a good vector for the Rosebery ore stratigraphic position at distal locations up to several hundred meters from ore; however, it should be noted that the S/Na_2O ratio may also be higher in pyritic shales that are unrelated to mineralization.

Ba/Sr ratio: This ratio reaches a peak in the ore zone alteration due to the fact that Ba substitutes for K in the white mica structure, whereas whole-rock Sr is depleted due to

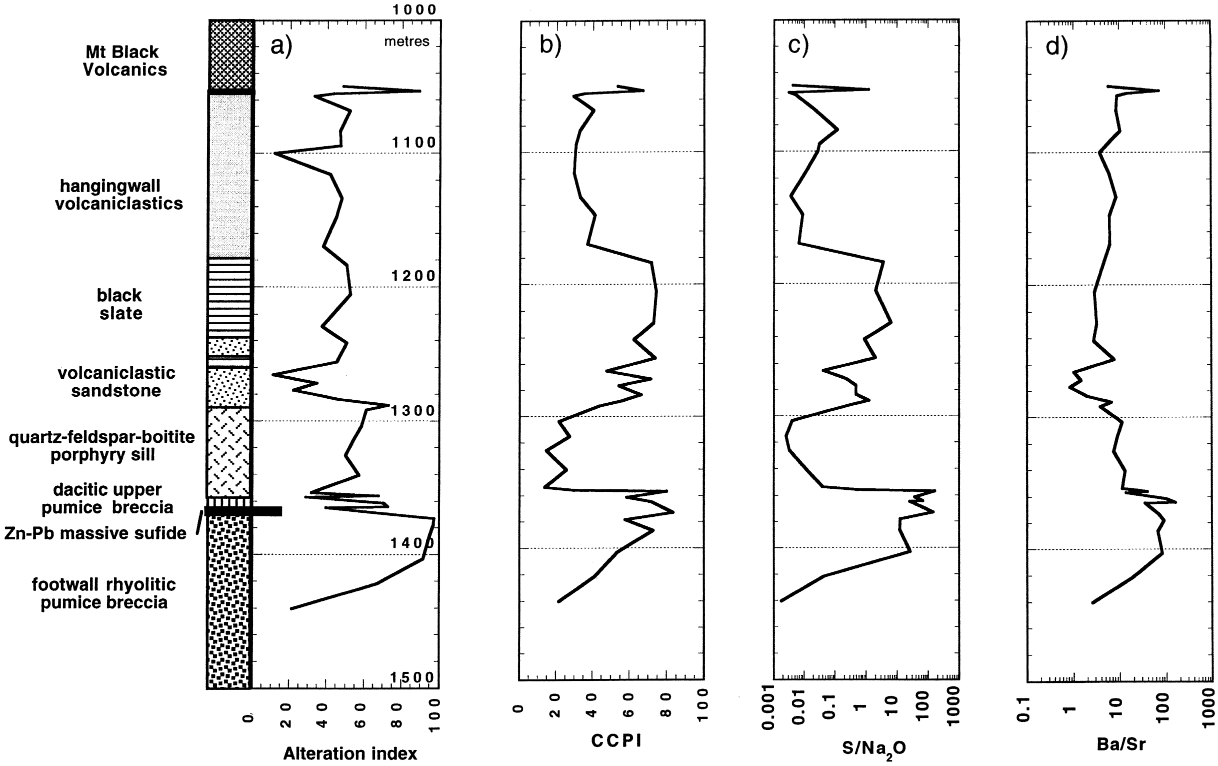

FIG. 11. Downhole plots of selected alteration indexes and element ratios for DDH 120R.

albite destruction. As shown in Figure 11 the Ba/Sr ratio increases abruptly through the footwall sericite and/or chlorite

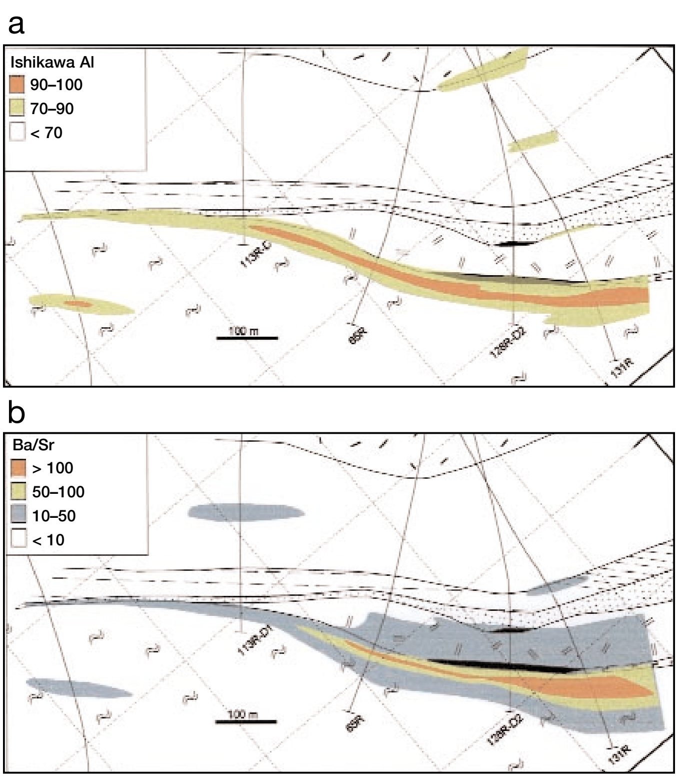

FIG. 12. Contoured geochemical indexes for section 1700 mN: (a) Ishikawa alteration index; (b) Ba/Sr. Geology key is same as Figure 2.

alteration zones, reaching a peak in the ore zone. A broad halo of elevated Ba/Sr extends up to 80 m into the hanging-wall sequence. This ratio is superior to most other indexes (but not thallium) in defining halos in the hanging wall directly above ore (Fig. 11) and for some distance lateral to ore (Fig. 12b) but becomes a less distinct vector at distal positions from ore. The Rb/Sr ratio (not shown) has a similar pattern to the Ba/Sr ratio but is less anomalous in the hanging-wall sequence.

Volatile element halos

Thallium and antimony are the only trace elements investigated in this study that show a clearly developed and widespread halo around the ore lenses. Smith and Huston (1992) previously reported significant Tl and Hg halos surrounding the ore lens at Rosebery; however, their sampling was limited and the full extent of the halos was not defined. In DDH 120R (Fig. 13) thallium exhibits an amazingly systematic pattern, defining a halo at least 270 m across stratigraphy surrounding the ore position. The halo of Tl in the hanging-wall units (porphyry sill, volcaniclastic sandstone, and black slate) varies systematically from >10 down to 1 ppm over a distance of 200 m, passing away from the orebody. The footwall halo is less widespead but extends at least 70 m below the ore lens. A second Tl peak occurs at the upper contact of the porphyry sill and/or volcanic sandstone (Fig. 13), suggesting a second zone of mineralization at this level (this mineralized position is confirmed in DDH 128R).

In section 1700 mN and the 17 level plan (Figs. 13, 14, 15) the thallium halo (above 1 ppm) forms an envelope about 200 to 300 m wide, which surrounds the ore lens and extends

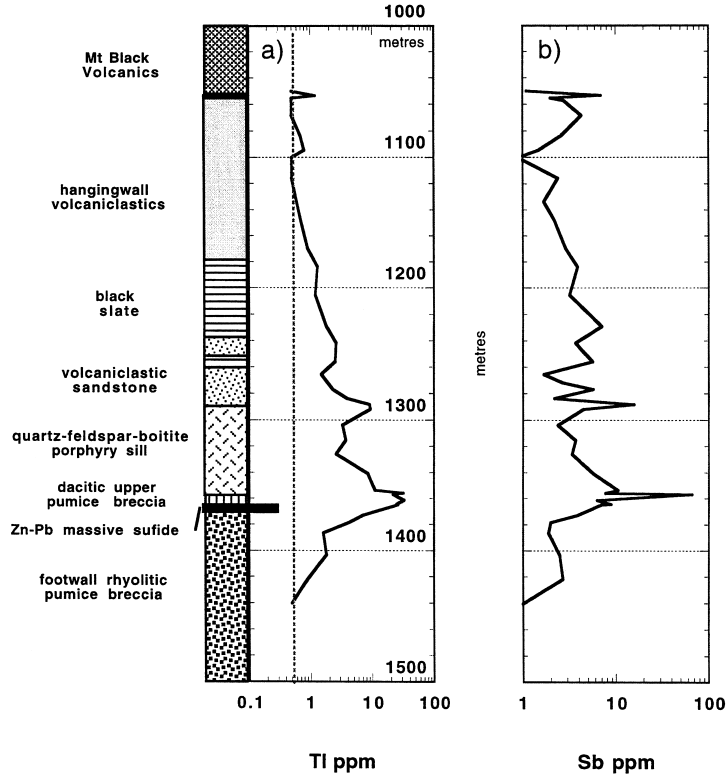

FIG. 13. Downhole plots of the volatile elements: Ti and Sb in DDH 120R.

along strike, defining the favorable ore position, for more than 500 m west (beyond DDH 109R). Regional studies in the Hercules area indicate that anomalous Tl values also occur at the White Spur Formation–Central Volcanic Complex contact 3.5 km south of the Hercules deposit. This research indicates that thallium may be effective in identifying regionally favorable ore horizons and locally, on the mine scale, to identify proximity to an ore lens.

Antimony shows a similar distribution to thallium outlining a broad halo around the ore lenses at Rosebery (Fig. 14b). However, Sb values tend to vary less systematically than thallium and it is therefore recommended that Sb should only be used in support of the Tl data rather than as an alternative to Tl. There is a good correlation between Tl and Sb for the complete Rosebery data set (Fig. 16), giving an indication of the variation in these trace elements throughout the halo to the K and A-B lenses.

Previous workers (e.g., Shaw, 1952; Ikramuddin et al., 1983) have concluded that Tl most likely substitutes for K-bearing minerals in the halo of base metal deposits. The data from Rosebery (not shown) exhibits a poor correlation between Tl and K_2O, suggesting that Tl is probably present in white mica in the alteration halo.

The extent of the TI halo up into the hanging-wall sedimentary and volcanic rocks may provide support for the subsurface replacement theory for Rosebery proposed by Allen (1994a). If the mineralization in the K lens formed by replacement of pumiceous volcanics below the quartz-porphyritic sill, then the volatile elements Tl and Sb may have been concentrated in the halo by the spent, hydrothermal fluids permeating the hanging-wall sequence. If this scenario is correct, the complete hanging-wall package, including the porphyry sill, volcaniclastic sandstones, black slate, and

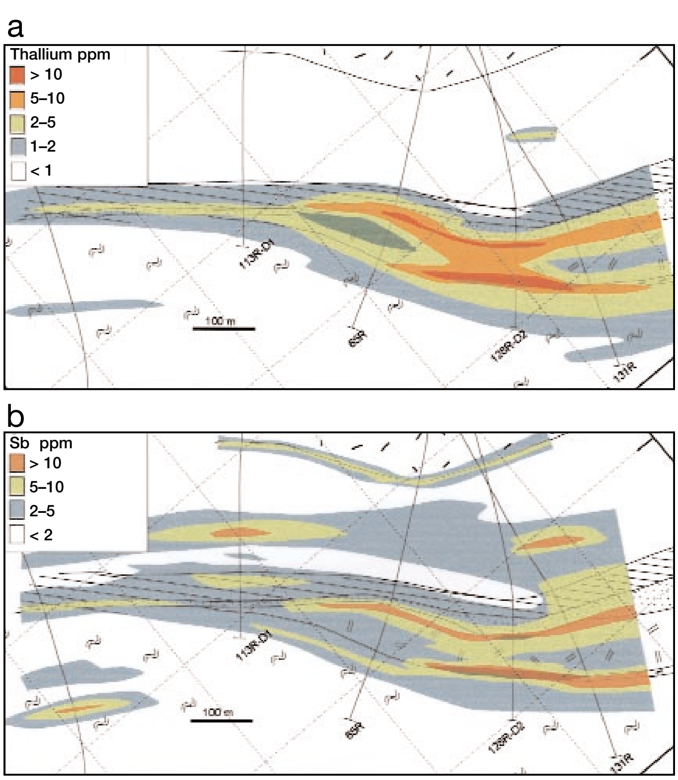

FIG. 14. Contoured geochemical data for (a) Tl, and (b) Sb in section 1700 mN.

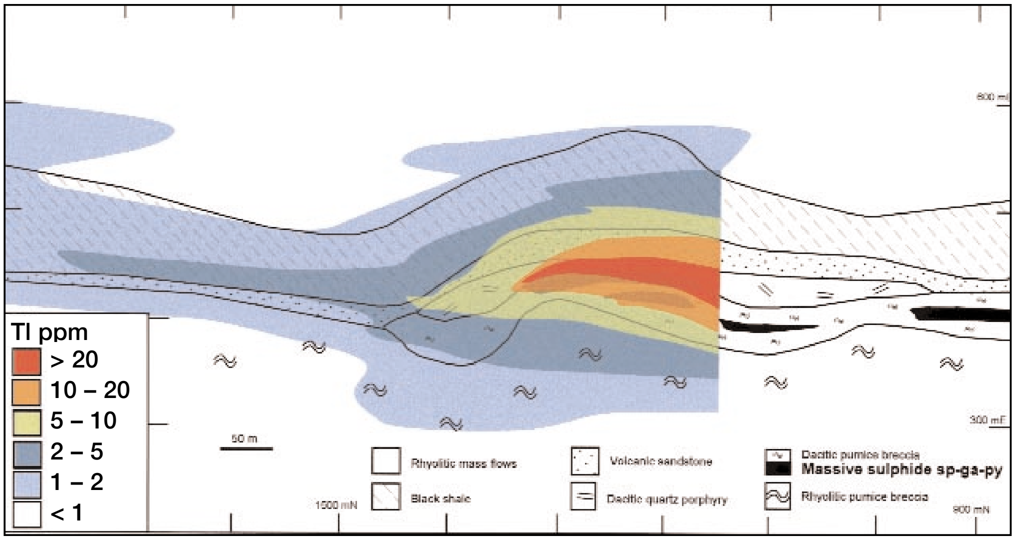

FIG. 15. Thallium distribution in the 17 level, Rosebery north end, using data from DDH R4452, 84R, 113RDI, and 109R.

hanging-wall volcaniclastic mass flows had to be in place prior to mineralization. An alternative explanation for the Tl, Sb halo is that it formed sometime later than the ore-forming event and was related to (1) a long-lived hydrothermal system that continued well after ore deposition, (2) shallow seawater circulation and diagenesis postmineralization, or (3) later metamorphism that caused redistribution of the most volatile elements, Tl and Sb, from the orebody into the surrounding host-rock package and overlying volcaniclastics.

Concurrent research on other Australian VHMS deposits—Thalanga (Paulick et al., 2001), Hellyer (Gemmell and Fulton, 2001), Western Tharsis (Huston and Kamprad, 2001), and Highway-Reward (Doyle, 2001)—indicates that the zinc-rich deposits at Rosebery, Hellyer, and Thalanga have the most extensive Tl and Sb halos, whereas, by comparison, the copper-rich deposits at Western Tharsis, Highway-Reward, and Gossan Hill have negligible Tl halos (Large et al., 2001). Of the zinc-rich VHMS deposits where data is available, Rosebery has the most extensive Tl halo; however, it is relatively small when compared to the regionally extensive Tl halos defined for Australian Proterozoic sediment-hosted

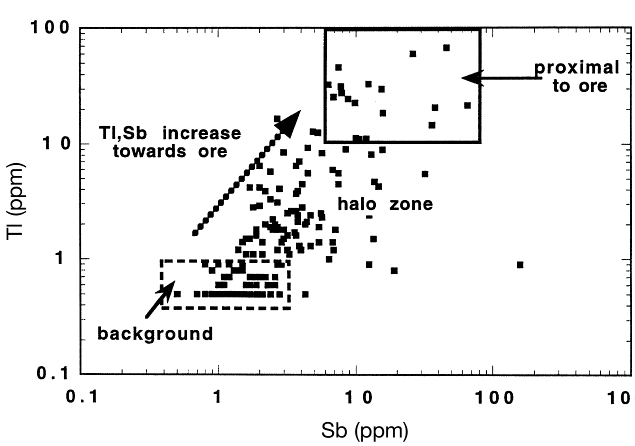

FIG. 16. Relationship between Tl and Sb for the ore zone and halo at Rosebery.

(SEDEX) Zn-Pb-Ag deposits, such as HYC (Smith, 1973; Large et al., 2000) and Lady Loretta (Large and McGoldrick, 1998).

Alteration Mineral Chemistry

A study of the variation in white mica, carbonate, and chlorite chemistry in two drill holes—DDH 120R through the center of the K lens (Fig. 2) and DDH 109R 500 m north of the K lens and A-B lens system—was undertaken in order to determine whether alteration mineral chemistry displays any zonal variation with respect to the position of the ore lenses at Rosebery. Additional studies were carried out by Herrmann et al. (2001) to evaluate the relationship between downhole PIMA spectra and white mica and chlorite composition at Rosebery as part of a general study of a number of VHMS systems.

White mica composition

White mica composition was determined for 129 white mica grains in 35 samples from DDH 120R and 109R. The downhole variation in DDH 120R for Fe + Mg cations, Na/(Na + K) ratio, and Ba cations is shown in Figure 17. Individual microprobe analyses are plotted as single points. In some samples only one white mica grain was analyzed, while other samples have multiple grain analyses. The spread of points at a given depth shows the variation in chemistry for several mineral grains from the same sample. The microprobe analyses (Fig. 17) indicate that Rosebery white mica chemistry can be divided into three groups:

1. Phengitic white micas with elevated Ba, which contain between 0.5 and 1.0 Fe + Mg cations substituting for octahedral Al, between 0.05 and 0.1 Ba ions substituting for K, and negligible Na. These white micas are found in the intensely altered dacitic upper pumice breccia horizon and within the strongly sericite altered footwall hydrothermal zone. The Ba content of the white mica is most elevated proximal to the ore lens, confirming a previous study by Gee (1970) on the composition of the ore zone white mica.

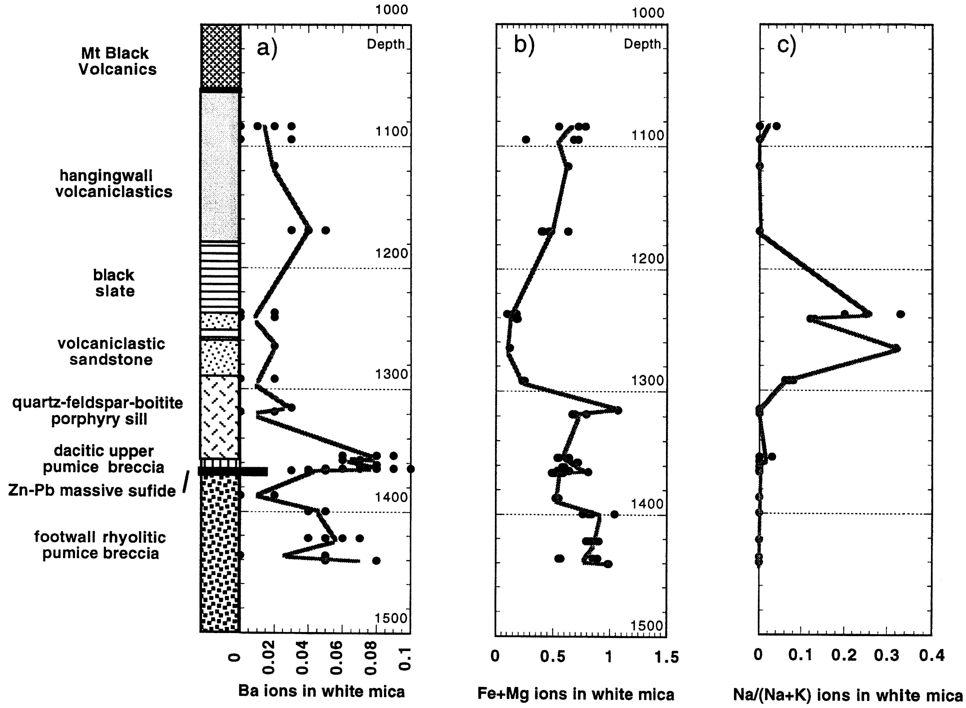

FIG. 17. Downhole variation in the composition of muscovite in DDH 120R: (a) Ba ions, (b) Fe + Mg ions, (c) Na/(Na + K) ions.

2. Phengitic white micas with negligible Ba, which are similar to the ore zone phengite but with Ba content less than 0.05 ions. These white micas occur in the weakly altered quartz-porphyriticsill overlying the ore lens and in the hanging-wall volcanics above the black slate. Their compositional range is similar to white micas from essentially unaltered volcanics found regionally away from mineralization in the Mount Read volcanic belt (Herrmann et al., 2001).

3. Sodic white micas with 0.05 to 0.35 Na/(Na + K) and low phengite content (<0.2 Fe + Mg cations). The Na exists as a substitution for K in white mica or in fine mixtures of paragonite and white mica. White micas of this type are restricted to the volcaniclastic sandstone unit overlying the quartz-porphyriticsill and underlying the black slate (Fig. 17). Further PIMA studies of the white mica compositional variation by Herrmann et al. (2001) indicate that the sodic white mica with Na/(Na + K) > 0.1 are restricted to the volcaniclastic sandstone unit immediately above the best development of mineralization in the K lens.

White micas from the remote hole DDH 109R are all group 2 phengites, suggesting that the barian and sodic white micas are restricted to the immediate ore environment. The only feature of white mica composition that is obviously related to mineralization is the increased substitution of Ba for K in close proximity to ore. Herrmann et al. (2001) also consider that the presence of sodic white mica is an indirect indicator of ore, with its distribution controlled by the more mafic host-rock composition of the volcanic sandstones, which are cofined to the volcano-sedimentary graben structure that ultimately controlled the position of the orebody.

Chlorite composition

Previous studies (e.g., Gill, 1976; McLeod and Stanton, 1984; Lydon, 1988; McLeod et al., 1987) have suggested that VHMS ores are commonly associated with more magnesium-rich chlorites compared to distal metamorphic chlorites. Averaged analyses of 83 chlorites in 22 samples from DDH 109R and 120R at Rosebery indicate compositions ranging in Mg number from 25 to 70 and in Si cations from 5.2 to 6.0 (Fig. 18). Chlorite compositional variations are not obviously related to intensity of hydrothermal alteration or spatially to sulfide lenses and the favorable horizon. However, the data are sparse, and there is a tendency for more Mg-rich chlorites to occur in the ore environment (dacitic upper pumice breccia and volcaniclastic sandstone). Chlorites associated with the sulfide lens in DDH 120R and in the anomalous hanging-wall volcaniclastic sandstone unit in both 120R and 109R have Mg numbers in the range of 50 to 70 (Fig. 19), compared to chlorites in the footwall and hanging-wall mass-flow units, which are more iron rich with Mg numbers in the range of 20 to 50. More chlorite analyses are required to confirm these trends.

Carbonate composition

Previous studies by Brathwaite (1974), Green et al. (1981), and Khin Zaw (1991) reported a manganese-rich suite of carbonates at Rosebery, including the following minerals in order of abundance: rhodochrosite ($MnCO_3$), ferroan rhodochrosite [(Mn,Fe) CO_3], kutnahorite [$CaMn(CO_3)_2$], manganoan siderite [Fe,(Mn) CO_3], dolomite [$CaMg(CO_3)_2$], and calcite ($CaCO_3$).

A total of 218 microprobe analyses of carbonate minerals from DDH 120R and 109R have been collected as part of this

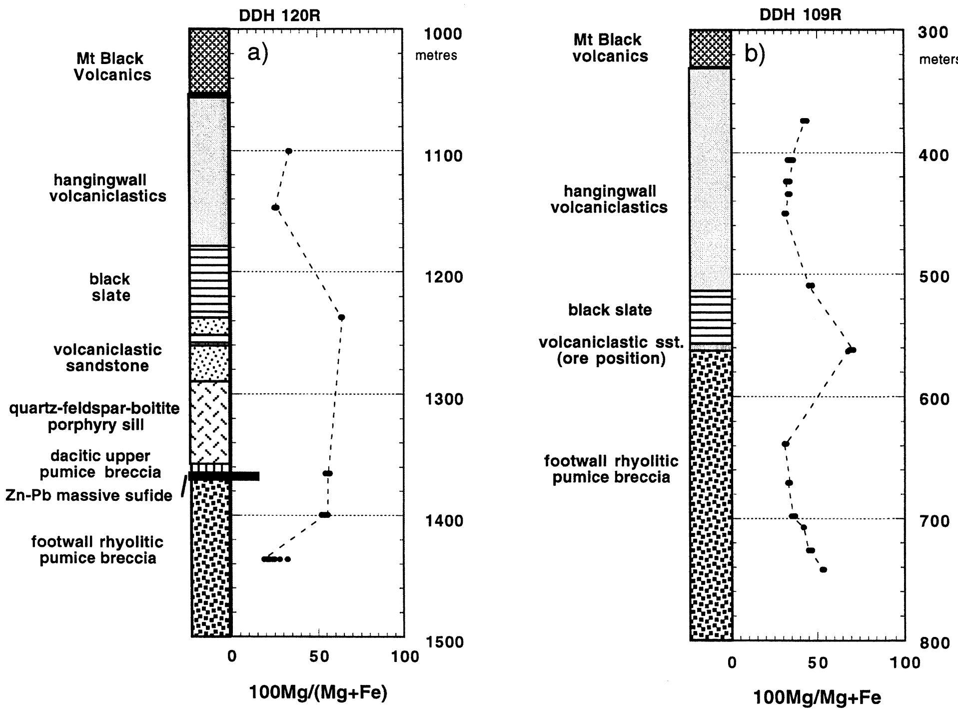

FIG. 18. Downhole variation in chlorite (100 Mg/(Mg + Fe)) from (a) DDH 120R, and (b) DDH 109R.

study. Data from DDH 120R, plotted in Figure 20, indicate that the carbonates fall into three main groups: (1) rhodochrosite-ferroan rhodochrosite with an $MnCO_3$ content from 45 to 95 mole percent, (2) ankerite-kutnahorite with an $MnCO_3$ content from 3 to 45 mole percent, and (3) calcite with an $MnCO_3$ content from 0 to 10 mole percent. Downhole variation in carbonate chemistry for DDH 120R (Fig. 21a) shows a clear spatial relationship of the Mn-rich carbonates with the ore zone and altered footwall. Carbonates within the ore lens and dacitic pumice breccia commonly contain greater than 20 mole percent $MnCO_3$, belonging to groups 1 and 2 above—rhodochrosite, ferroan-rhodochrosite, and ferroan-kutnahorite. Carbonates in the footwall alteration zone are similar to those in the ore zone but are commonly at the Fe-rich end of the spectrum—ferroan-rhodochrosite, ankerite, and rarely siderite (Fig. 20). In contrast, the hanging-wall rocks overlying the quartz-porphyriticsill contain calcite only, with a low Mn, Fe, and Mg content (less than 3 mole % of $MnCO_3$, $FeCO_3$, and $MgCO_3$). The most Fe-Mn poor calcites are found in the hanging-wall volcaniclastic sandstone unit, which is also host to the most Fe-Mn poor white mica.

Microprobe analyses of carbonates in DDH 109R, 500 m to the west of the ore lenses (Fig. 2), indicate the ubiquitous presence of calcite with less than 3 mole percent $MnCO_3$ and $FeCO_3$. There does not appear to be any development of $MnCO_3$ at the ore position (top of the rhyolitic pumice breccia or the overlying volcaniclastic sandstones) in this drill hole. However manganoan siderite with 25 to 45 mole percent $MnCO_3$ is present as a series of carbonate-arsenopyrite–pyrite

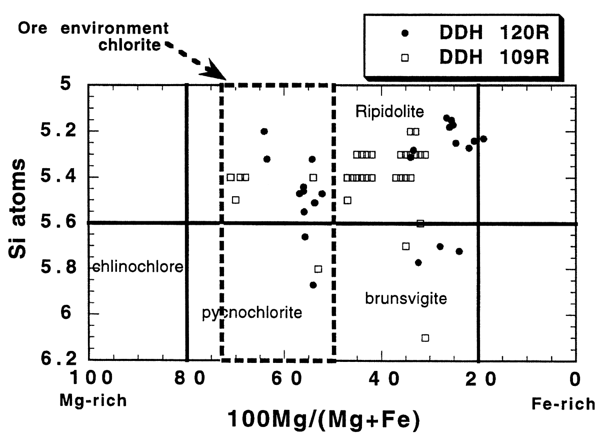

FIG. 19. Variation in composition of chlorites from Rosebery.

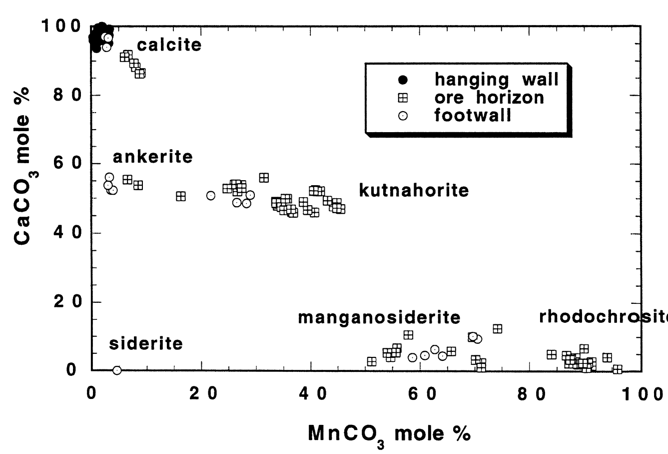

FIG. 20. Composition of carbonates from DDH 120R showing the separation into three major groups.

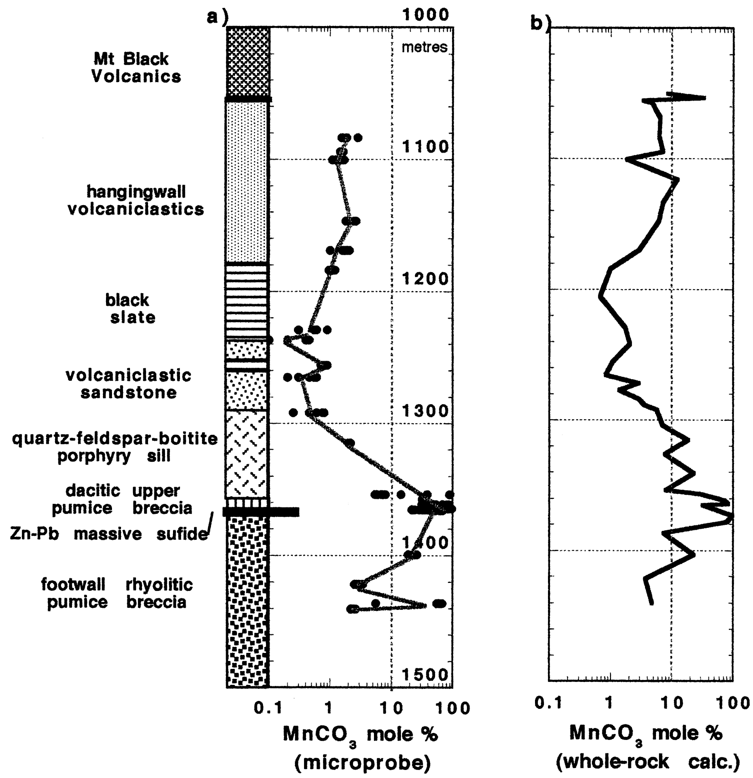

FIG. 21. Downhole variation in $MnCO_3$ content in DDH 120R: (a) from microprobe data, (b) calculated from whole-rock analyses as described in the text.

veins with associated alteration deep in the footwall 160 m below the ore position.

In order to further test the use of carbonate composition as an exploration vector to mineralization, a comparison was attempted between the microprobe analyses on carbonates and the composition calculated from whole-rock analyses. This approach was taken because whole-rock analyses are a more common and less costly data set used in mineral exploration than detailed downhole microprobe analyses. A similar method has been previously used by Large and McGoldrick (1998) and Large et al. (2000) in the study of Mn carbonate halos associated with stratiform sediment-hosted Zn-Pb-Ag deposits. This procedure assumes that all of the whole-rock MnO is present within manganese carbonate minerals. This is a partly valid assumption for the Rosebery area, although very minor MnO is present in chlorite. The relationship used for estimating $MnCO_3$ mole percent from whole-rock data is $MnCO_3$ mole percent $= \frac{MnO_{wr}/71.8}{CO_{2wr}/44}$, where MnO_{wr} and CO_{2wr} are the whole-rock analyses of these components. A comparison of the downhole $MnCO_3$ variation between microprobe and whole-rock data for DDH 120R is shown in Figure 21. These plots show very similar trends and demonstrate that useful information is available from the whole-rock calculation method. For DDH 120R (Fig. 21b) the whole-rock calculation shows that mole percent $MnCO_3$ is an excellent vector to mineralization, increasing gradually over a 100-m interval (1,220–1,320 m) down toward the ore lens through the hanging-wall volcaniclastic sandstones and the quartz-porphyriticsill. Caution should be used when applying this approach to other ore systems, especially in intermediate or mafic host rocks, where Mn chlorite is most likely to be a significant component.

Halo Model for Rosebery

A composite halo model has been developed for the Rosebery AB and K lenses based on the alteration mineralogy, mineral chemistry, and element dispersions presented above for the nine drill holes studied (Fig. 22). The major features of the halo model are the following:

1. Sericite is the most extensive hydrothermal phase related to mineralization. Sericite forms an envelope that is best developed in the footwall volcanics and surrounding the thickest massive sulfide intersections. The zone of sericite alteration is strata bound at the top contact of the footwall pumice breccias, diminishing in intensity and thickness along the favorable stratigraphy over 500 m from the edge of the ore lenses. Adjacent to the ore lenses, the sericite has phengitic compositions with elevated Ba, while in laterally distal locations within the halo the sericite is Ba-poor phengite. Sodic white mica is concentrated in the hanging-wall volcaniclastic sandstones above the best development of massive sulfides.

2. Mn carbonate is disseminated within the sericite alteration halo and is an excellent indicator of proximity to ore. Massive Mn carbonate (rhodochrosite, ferroan-rhodochrosite, kutnahorite) is developed close to the ore lenses, especially in the immediate hanging wall within the dacitic upper pumice breccia, while spotted carbonate exists as a replacement phase in more distal locations. The Mn content of the carbonate

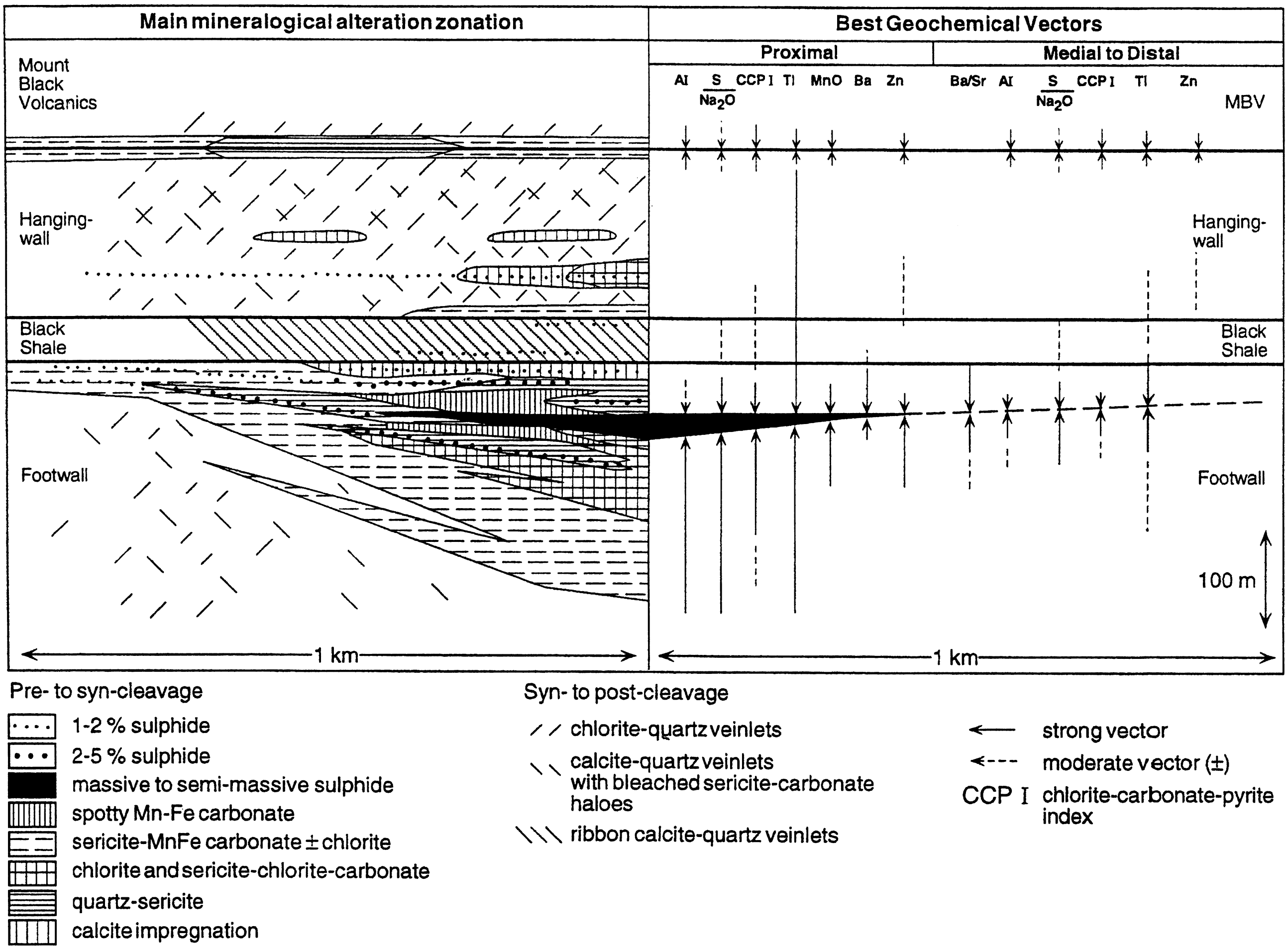

FIG. 22. Rosebery B-K lens alteration model and stratigraphic extent of the principal geochemical vectors.

increases toward ore from both the hanging-wall and footwall sides of the lenses, over distances of up to 200 m. Beyond the Mn carbonate halo the dominant background (metamorphic) carbonate mineral is Mn-Fe-poor calcite.

3. Hydrothermal chlorite is confined to the immediate footwall of the ore lens and is best developed below the Cu-rich parts of the mineralization. Chlorite forms the center of the sericite-Mn carbonate alteration halos. Limited microprobe data indicate that the chlorite composition is not spatially related to mineralization, although chlorites in the host unit tend to be more Mg rich (Mg no. from 50–75).

4. The ore elements, Zn, Pb, and Cu, are relatively tightly constrained, exhibiting limited halos around the ore lenses and along the favorable stratigraphic horizon. However, a zone of low-level Zn anomalism is developed in the uppermost hanging-wall volcaniclastics and, although disconnected from the ore-related zinc anomaly, may have some relationship to the Rosebery hydrothermal system—e.g., weak late-stage postore hydrothermal mineralization from the same vent system.

5. Thallium and antimony form the most extensive trace element dispersion halos surrounding the A-B-K lenses. Anomalous levels of these elements extend beyond the sericite alteration and Mn carbonate halos, into the hanging-wall volcaniclastics, and along the favorable stratigraphy greater than 500 m and beyond the limits of sampling.

No footwall alteration pipes or hydrothermal feeder zones have been defined below the A-B or K lenses in the present study. This suggests four possibilities: (1) discrete feeder channels did not exist, but instead the hydothermal solutions permeated upward through the porous footwall pumice-rich volcanics giving rise to the pervasive sericite-bearing footwall alteration; (2) feeder channels did exist but there is insufficient drilling below the ore stratigraphic level to define the channels; (3) the feeder channels have been transformed subparallel to bedding and cleavage during the intense deformation that affected the Rosebery south-end ore lenses (Large, 1990, figs. 6 and 7), and (4) the feeder channels are in an unknown distal location, and the fluids moved laterally along the top contact of the footwall pumice breccias to form the ore lenses. Further work is underway to resolve these possibilities.

Exploration vectors

The stratigraphic and lateral extent of a number of potentially useful geochemical exploration vectors that were tested in this study are shown in Figure 22. In summary the geochemical vectors are grouped according to their position within the overall halo system.

Proximal vectors: Zn, Pb, Ba, whole-rock MnO, Ba content of white mica are useful in the detection of ore lenses within 200 to 300 m along strike and 5 to 50 m across strike.

Medial vectors: Na_2O depletion, K_2O, Ishikawa AI, CCPI, S/Na_2O ratio, Ba/Sr ratio, Mn content of carbonate are useful in the detection of ore lenses within 300 to 500+ m along strike, 10 to 80 m into the hanging wall, and 60 to 120 m into the footwall.

Distal vectors: Tl and Sb are useful in the detection of ore for more than 500 m along strike from ore lenses, 200 to 300 m into the hanging wall, and 60 to 100 m into the footwall.

A diagramatic sketch showing the extent of some proximal vectors (Zn, Pb, Mn halo), medial vector (Ba/Sr ratio), and distal vectors (Tl, Sb halo) is given in Figure 23.

Acknowledgments

Special thanks to Pasminco management and staff for providing access and support to enable this project to proceed. Thanks also to Australian Mineral Industry Research Association (AMIRA) for coordinating the P439 project, to the Australian Research Council for providing financial support through the SPIRT scheme, and to the following companies that supported P439: Aberfoyle, RGC Exploration, Normandy, Rio Tinto, Pasminco, Deenhurst, Queensland Metals, and Mineral Resources Tasmania.

REFERENCES

Allen, R.L., 1994a, Syn-volcanic, subseafloor replacement model for Rosebery and other massive sulfide ores [ext. abs.]: Contentious Issues in Tasmanian Geology Symposium, Geological Society of Australia Tasmanian Division, Extended Abstracts Volume, p. 89–91.

——1994b, Volcanic facies analysis indicates large pyroclastic eruptions, sill complexes, syn-volcanic grabens, and subtle thrusts in the Cambrian "Central Volcanic Complex" volcanic centre, western Tasmania [ext. abs.]: Contentious Issues in Tasmanian Geology Symposium, Geological Society of Australia Tasmanian Division, Extended Abstracts Volume, p. 31–32.

——1997, Rosebery alteration study and regional alteration studies in the Mount Read Volcanics: The record of diagenetic alteration in the strongly deformed, felsic volcaniclastic succesion enclosing the Rosebery and Hercules massive sulfide deposits: Australian Mineral Industry Research Association (AMIRA) project P439, Unpublished report 5, October 1997, p. 135–145.

Allen, R.L., and Cas, R.A.F., 1990, The Rosebery controversy: Distinguishing prospective submarine ignimbrite-like units from true subaerial ignimbrites in the Rosebery-Hercules Zn-Cu-Pb massive sulfide district, Tasmania [abs.]: Australian Geological Convention, 10th, Hobart, Geological Society of Australia, Abstracts, p. 31–32.

Barrett, T.J., Thompson, J.F.H., and Sherlock, R.L., 1996, Stratigraphic, lithogeochemical and tectonic setting of the Kutcho Creek massive sulfide deposit, northern British Columbia: Exploration and Mining Geology, v. 5, p. 309–338.

Berry, R.F., and Keele, R.A., 1997, Cambrian tectonics and mineralization in western Tasmania: International Mining Geology Conference, 3rd, Launceston, November 1997, Australasian Institute of Mining and Metallurgy, Proceedings, p. 13–16.

Brathwaite, R.L., 1972, The structure of the Rosebery ore deposit, Tasmania: Australasian Institute of Mining and Metallurgy, Proceedings, no. 241, p. 1–13.

——1974, The geology and origin of the Rosebery ore deposit, Tasmania: ECONOMIC GEOLOGY, v. 69, p. 1086–1101.

Crawford, A.J., Corbett, K.D., and Everard, J.L., 1992, Geochemistry of the Cambrian volcanic-hosted massive sulfide-rich Mount Read Volcanics, Tasmania, and some tectonic implications: ECONOMIC GEOLOGY,v. 87, p. 597–619.

Doyle, M.G., 2001, Volcanic influences on hydrothermal and diagenetic alteration: Evidence from the Highway-Reward deposit, Mount Windsor subprovince, Australia: ECONOMIC GEOLOGY, v. 96, p. 1133–1148.

Gee, C.E., 1970, The geochemistry of some black shales in relation to the origin of certain stratiform ore deposits in Tasmania: Unpublished Ph.D. thesis, Hobart, Tasmania, University of Tasmania, 205 p.

Gemmell, J.B., and Fulton, R., 2001, Geology, genesis, and exploration implications of the footwall and hanging-wall alteration associated with the Hellyer volcanic-hosted massive sulfide deposit, Tasmania, Australia: ECONOMIC GEOLOGY, v. 96, p. 1003–1035.

Gifkins, C.C., and Allen, R.L., 2001, Textural and chemical characteristics of diagenetic and hydrothermal alteration in glassy volcanic rocks: Examples from the Mount Read Volcanics, Tasmania: ECONOMIC GEOLOGY, v. 96, p. 973–1002.

Gill, J.W., 1976, The Takiyuak metavolcanic belt: Geology, geochemistry and mineralisation: Unpublished Ph.D. thesis, Ottawa, Canada, Carleton University, 210 p.

Goodfellow, W.D., and Peter, J.M., 1994, Geochemistry of hydrothermally altered sediment, Middle Valley, northern Juan de Fuca Ridge: Proceedings of the Ocean Drilling Program, Scientific Results, v. 139, p. 207–290.

Green, G.R., and Iliff, G.D., 1989, Rosebery: Geological Society of Australia Special Publication 15, p. 132–137.

Green, G.R., Solomon, M., and Walshe, J.L., 1981, The formation of the volcanic-hosted massive sulfide ore deposit at Rosebery, Tasmania: ECONOMIC GEOLOGY, v. 76, p. 304–338.

Herrmann, W., Blake, M., Doyle, M., Huston, D., Kamprod, J., Merry, N., and Pontual, S., 2001, Short wavelength infrared (SWIR) spectral analysis of hydrothermal alteration zones associated with base metal sulfide deposits

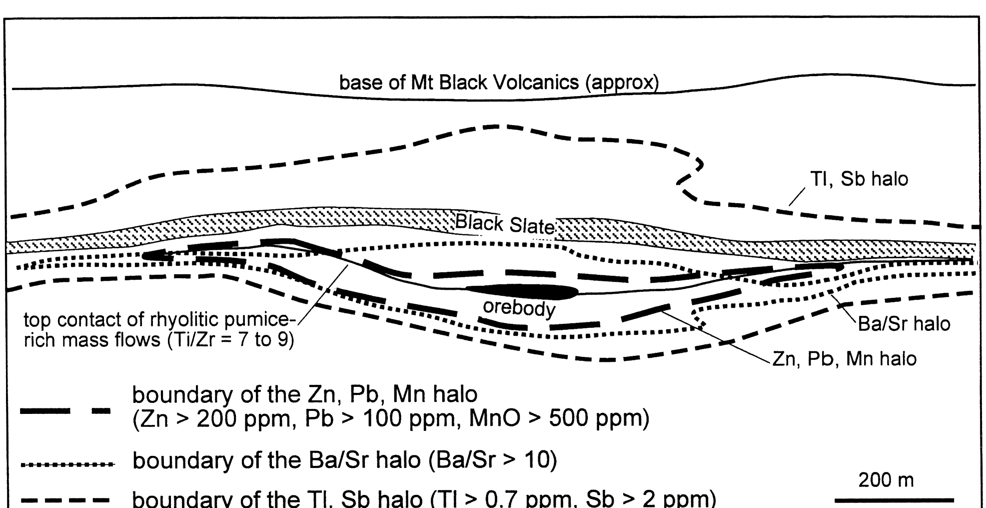

FIG. 23. Diagrammatic representation of the extent of three of the most useful exploration vectors at Rosebery (based on the B-K lens).

at Rosebery and Western Tharsis, Tasmania, and Highway-Reward, Queensland: ECONOMIC GEOLOGY, v. 96, p. 939–955.
Huston, D.L., and Kamprad, J., 2001, Zonation of alteration facies at Western Tharsis: Implications for the genesis of Cu-Au deposits in the Mount Lyell field, western Tasmania: ECONOMIC GEOLOGY, v. 96, p. 1123–1132.
Huston, D.L., and Large, R.R., 1987, The distribution, mineralogy and geochemistry of gold and silver in the north-end orebody, Rosebery mine, Tasmania: ECONOMIC GEOLOGY, v. 83, p. 1181–1192.
Ikramuddin, M., Asmeron, Y., Nordstrom, P.M., Kinart, K.P., Martin, W.M., Digby, S.J.M., Elder, D.D., Nijak, W.F., and Afemari, A.A., 1983, Thallium: A potential guide to mineral deposits: Journal of Geochemical Exploration, v. 19, p. 465–490.
Ishikawa, Y., Sawaguchi, T., Iwaya, S., and Horiuchi, M., 1976, Delineation of prospecting targets for Kuroko deposits based in modes of volcanicsm of underlying dacite and alteration halos: Mining Geology, v. 26, p. 105–117 (in Japanese with English abs.).
Khin Zaw, 1991, The effect of Devonian metamorphism and metasomatism on the mineralogy and geochemistry of the Cambrian VMS deposits in the Rosebery-Hercules district, western Tasmania: Unpublished Ph.D. thesis, Hobart, Tasmania, University of Tasmania, 342 p.
Khin Zaw, Large, R.R., and Huston, D.L, 1997, Petrological and geochemical significance of a Devonian replacement zone in the Cambrian Rosebery VHMS deposit, western Tasmania: Canadian Mineralogist, v. 35, p. 1325–1350.
Khin Zaw, Huston, D.L., and Large, R.R., 1999, A chemical model for the Devonian remobilization process in the Cambrian volcanic-hosted massive sulfide Rosebery deposit, western Tasmania: ECONOMIC GEOLOGY, v. 94, p. 529–546.
Large, R.R., 1990, The gold-rich sea-floor massive sulfide deposits of Tasmania: Geologische Rundshau, v. 79, p. 256–278.
——1992, Australian volcanic-hosted massive sulfide deposits: Features, styles and genetic models: ECONOMIC GEOLOGY, v. 87, p. 471–510.
Large, R.R., and McGoldrick, P.J., 1998, Lithogeochemical halos and geochemical vectors to stratiform sediment hosted Zn-Pb-Ag deposits. Part 1: Lady Loretta deposit, Queensland: Journal of Geochemical Exploration, v. 63, p. 37–56.
Large, R.R., Bull, S.W., and McGoldrick, P.J., 2000, Lithogeochemical halos and geochemical vectors to stratiform sediment hosted Zn-Pb-Ag deposits. Part 2: HYC deposit, McArthur River, Northern Territory: Journal of Geochemical Exploration, v. 68, p. 105–126.
Large, R.R., Gemmell, J.B., Paulick, H., and Huston, D.L., 2001, The alteration box plot: A simple approach to understanding the relationship between alteration mineralogy and lithogeochemistry associated with volcanic-hosted massive sulfide deposits: ECONOMIC GEOLOGY, v. 96, p. 957–971.
Lydon, J.W., 1988, Ore deposit models #14. Volcanogenic massive sulfide deposits Part 2: Genetic models: Geoscience Canada, v. 15, p. 43–65.
MacLean, W.H., and Barrett, T.J., 1993, Lithogeochemical techniques using immobile elements: Journal of Geochemical Exploration, v. 48, p. 109–133.
McLeod, R.L., and Stanton, R.L., 1984, Phyllosilicates and associated minerals in some Paleozoic stratiform sulfide deposits of southeastern Australia: ECONOMIC GEOLOGY, v. 79, p. 1–22.
McLeod, R.L., Gabell, A.R., Green, A.A., and Gardavsky, V., 1987, Chlorite infrared spectral data as proximity indicators of volcanogenic massive sulfide mineralisation: Pacific Rim Congress 87, Gold Coast, August 1987, Australasian Institute of Mining and Metallurgy, Proceedings, p. 321–324.
Naschwitz, W., and Van Moort, J.C., 1991, Geochemistry of wallrock alteration, Rosebery, Tasmania, Australia: Applied Geochemistry, v. 6, p. 267–278.
Paulick, H., Herrmann, W., and Gemmell, J.B., 2001, Alteration of felsic volcanics hosting the Thalanga massive sulfide deposit, North Queensland, Australia: Geochemical proximity indicators to ore: ECONOMIC GEOLOGY, v. 96, p. 1175–1200.
Pwa, A., Naschwitz, W., Hotchkis, M., and Van Moort, J.C., 1992, Exploration rock geochemistry in the Rosebery mine area, western Tasmania: Tasmanian Department Mines, Geological Survey Bulletin, v. 70, p. 7–16.
Reid, L.G., 1993, Aspects of north-end mineralisation, Rosebery mine, western Tasmania: Unpublished M.Sc. thesis, Hobart, Tasmania, University of Tasmania, 82 p.
Shaw, D.M., 1952, The geochemistry of thallium: Geochimica et Cosmochimica Acta, v. 2, p. 118–154.
Smith, R.N., 1973, Trace element distributions within some major stratiform orebodies: Unpublished B.Sc. Honors thesis, Parkville, Victoria, University of Melbourne, 189 p.
Smith, R.N., and Huston, D.L., 1992, Distribution and association of selected trace elements at the Rosebery deposit, Tasmania: ECONOMIC GEOLOGY, v. 87, p. 706–719.
Whitford, D.J., McPherson, W.P.A., and Wallace, D.B., 1989, Geochemistry of the host rocks of the volcanogenic massive sulfide deposit at Que River, Tasmania: ECONOMIC GEOLOGY, v. 84, p. 1–21.